Joint International Topical Meeting on Mathematics & Computation and Supercomputing in Nuclear Applications (M&C + SNA 2007)
Monterey, California, April 15-19, 2007, on CD-ROM, American Nuclear Society, LaGrange Park, IL (2007)

Sensitivity analysis of the kinetic behaviour of a Gas Cooled Fast Reactor to variations of the delayed neutron parameters

W.F.G. van Rooijen*and D. Lathouwers
Delft University of Technology,
R^3 / PNR
Mekelweg 15, 2629 JB Delft
The Netherlands
w.f.g.vanrooijen@tudelft.nl

ABSTRACT

In advanced Generation IV (fast) reactors an integral fuel cycle is envisaged, where all Heavy Metal is recycled in the reactor. This leads to a nuclear fuel with a considerable content of Minor Actinides. For many of these isotopes the nuclear data is not very well known. In this paper the sensitivity of the kinetic behaviour of the reactor to the dynamic parameters λ_k, β_k and the delayed spectrum $\chi_{d,k}$ is studied using first order perturbation theory. In the current study, feedback due to Doppler and/or thermohydraulic effects are not treated. The theoretical framework is applied to a Generation IV Gas Cooled Fast Reactor. The results indicate that the first-order approach is satisfactory for small variations of the data. Sensitivities to delayed neutron data are similar for increasing and decreasing transients. Sensitivities generally increase with reactivity for increasing transients. For decreasing transients, there are less clearly defined trends, although the sensitivity to the delayed neutron spectrum decreases with larger sub-criticality, as expected. For this research, an adjoint capable version of the time-dependent diffusion code DALTON is under development.

Key Words: Gas Cooled Fast Reactor, Adjoint Sensitivity Analysis Procedure, delayed neutron parameters, DALTON

1. Theory

In this paper first order perturbation theory is used to calculate the sensitivity of a transient to nuclear data. Earlier examples of the application of perturbation theory to delayed neutron data are Kiefhaber [1992], where the effect of data errors on (measured) static reactivity is treated. We choose an approach similar to Onega and Florian [1983], to calculate the sensitivity of an actual transient to delayed neutron data. Transient neutronics codes, like EVENT (de Oliveira and Goddard [1996]) or DORT-TD (Pautz and Birkhofer [2003]), are becoming more widely available and the applied formalism can be readily implemented as a postprocessor using forward and adjoint time-dependent flux solutions computed by such codes. The approach is to calculate a transient in a nuclear reactor, and then determine how the evolution of the reactor power depends on the delayed neutron data. To this end, we start out by defining a response quantity R, which in this case is (an integral over) the total power of the reactor:

$$R(\alpha,\phi) = \int_V \int_0^\infty \int_0^{t_f} [E_{\text{rel}}(\mathbf{r},E,t)\Sigma_f(\mathbf{r},E,t)\phi(\mathbf{r},E,t)]h(\mathbf{r},t)dtdEd\mathbf{r} \tag{1}$$

*Corresponding author, current address: Nuclear Reactor Engineering and Medical Physics program, Woodruff School of Mechanical Engineering, Georgia Tech, 801 Ferst Drive, N.W. Atlanta, GA 30332-0405 USA

where α indicates data (parameters) pertaining to the problem, like $\beta_k, \lambda_k, \Sigma_f, E_{\text{rel}}$ etc, $\phi = \phi(\alpha)$ is the flux and E_{rel} is the energy release per fission. $h(\mathbf{r}, t)$ is a weight function, for instance to select the response at a certain position and time. Small variations of the data $\alpha = \alpha^0 + \delta\alpha$ will cause a perturbation of the time dependent flux during the transient. Using a multi-group formalism, and treating E_{rel}, Σ_f as data, the perturbed response in multi-group notation is found by taking the Gâteaux-differential of (1):

$$\delta R = \lim_{\epsilon \to 0} \frac{d}{d\epsilon} \int_V \int_0^{t_f} \sum_{g=1}^{G} [(E^g_{\text{rel}} + \epsilon \delta E^g_{\text{rel}})(\Sigma^g_f + \epsilon \delta \Sigma^g_f)(\phi^g + \epsilon \delta \phi^g)] h(\mathbf{r}, t) dt d\mathbf{r} \tag{2}$$

which can be expanded to give (note that the Gâteaux-differential leaves only first-order terms):

$$\begin{aligned} \delta R = &\int_V \int_0^{t_f} \sum_{g=1}^{G} [\delta E^g_{\text{rel}} \Sigma^g_f \phi^g] h(\mathbf{r}, t) dt d\mathbf{r} + \int_V \int_0^{t_f} \sum_{g=1}^{G} [E^g_{\text{rel}} \delta \Sigma^g_f \phi^g] h(\mathbf{r}, t) dt d\mathbf{r} + \dots \\ &\dots + \int_V \int_0^{t_f} \sum_{g=1}^{G} [E^g_{\text{rel}} \Sigma^g_f \delta \phi^g] h(\mathbf{r}, t) dt d\mathbf{r} \end{aligned} \tag{3}$$

It is seen that δR is a sum of two 'direct' effects due to (known) data perturbations δE^g_{rel} and $\delta \Sigma^g_f$, and an 'indirect' effect due to the flux perturbation $\delta \phi^g$. In this paper only perturbations of delayed neutron data are considered, hence the δE^g_{rel} and $\delta \Sigma^g_f$ terms are treated as zero. To obtain $\delta \phi^g$, the forward diffusion equation could be solved repeatedly for each parameter variation $\delta\alpha$. However, a more elegant approach is to employ the Adjoint Sensitivity Analysis Procedure (ASAP) as described in Cacuci [2003]. Doing so, all terms involving $\delta \phi^g$ in δR are replaced by terms involving perturbations of the data $\delta\alpha$ and the adjoint flux ϕ^{g+}. This approach is comparable to that described in Onega and Florian [1983]. In van Rooijen [2006], van Rooijen et al. [2007] a similar approach is used for nuclide transmutation theory.

In a multi-group diffusion approach, the forward flux is found as the solution of the multi-group diffusion equation (for G neutron energy groups and K precursor families for delayed neutrons):

$$\frac{1}{v_g} \frac{\partial \phi^g}{\partial t} - \nabla \cdot D^g \nabla \phi^g + \Sigma^g_t \phi^g = \sum_{g'=1}^{G} \Sigma^{g' \to g}_s \phi^{g'} + \chi^g_p (1 - \beta) \sum_{g'=1}^{G} \nu \Sigma^{g'}_f \phi^{g'} + \sum_{k=1}^{K} \lambda_k C_k \chi^g_{d,k} \tag{4}$$

$$\frac{\partial C_k}{\partial t} = \beta_k \sum_{g=1}^{G} \nu \Sigma^g_f \phi^g - \lambda_k C_k \tag{5}$$

$$\phi^g|_{\mathbf{r}, t \leq 0} = \phi^g(\mathbf{r}, 0) \tag{6}$$

$$C_k|_{\mathbf{r}, t \leq 0} = \frac{\beta_k}{\lambda_k} \sum_{g=1}^{G} \nu \Sigma^g_f(\mathbf{r}) \phi^g(\mathbf{r}, 0) \tag{7}$$

where it is assumed that the reactor is critical at steady state, and appropriate spatial boundary conditions are implicitly assumed. If the dynamic parameters β_k, λ_k and $\chi_{d,k}$ are treated as data, the governing equations for the flux perturbations are found by taking the Gâteaux-differentials of equations (4) to (7).

After carrying through the differentiations to ϵ and taking the limit for ϵ to zero, the resulting equations can be rearranged to give the following:

$$\frac{1}{v^g}\frac{\partial \delta\phi^g}{\partial t} - \nabla \cdot D^g \nabla \delta\phi^g + \Sigma_t^g \delta\phi^g - \sum_{g'=1}^{G} \Sigma_s^{g' \to g} \delta\phi^{g'} - \chi_p^g (1-\beta) \sum_{g'=1}^{G} \nu\Sigma_f^{g'} \delta\phi^{g'} - \sum_{k=1}^{K} \lambda_k \chi_{d,k}^g \delta C_k = \chi_p^g \left(\sum_{k=1}^{K} (-\delta\beta_k) \right) \sum_{g'=1}^{G} \nu\Sigma_f^{g'} \phi^{g'} + \sum_{k=1}^{K} \delta\lambda_k \chi_{d,k}^g C_k + \sum_{k=1}^{K} \lambda_k \delta\chi_{d,k}^g C_k \quad (8)$$

$$\frac{\partial \delta C_k}{\partial t} - \beta_k \sum_{g=1}^{G} \nu\Sigma_f^g \delta\phi^g + \lambda_k \delta C_k = \delta\beta_k \sum_{g=1}^{G} \nu^g \Sigma_f^g \phi^g - \delta\lambda_k C_k \quad (9)$$

$$\delta\phi^g|_{\mathbf{r},t=0} = \delta\phi^g(\mathbf{r},0) \quad (10)$$

$$\delta C_k|_{\mathbf{r},t=0} = \frac{\lambda_k \delta\beta_k - \beta_k \delta\lambda_k}{\lambda_k^2} \sum_{g=1}^{G} \nu\Sigma_f^g \phi^g(\mathbf{r},0) + \frac{\beta_k}{\lambda_k} \sum_{g=1}^{G} \nu\Sigma_f^g \delta\phi^g(\mathbf{r},0) \quad (11)$$

Equations 8 to 11 could be used to solve for the flux perturbation $\delta\phi^g$, but since each data perturbation requires a new calculation, the effort would be the same as for simply recalculating the entire transient with perturbed data. Introducing the vector $\Psi(\mathbf{r},t) = [\phi^1(\mathbf{r},t), \ldots, \phi^G(\mathbf{r},t), C_1(\mathbf{r},t), \ldots, C_K(\mathbf{r},t)]^T$ (column vector) and its adjoint counterpart $\Psi^+(\mathbf{r},t)$, it is possible to use equations 8 and 9 to substitute the terms involving $\delta\phi^g$ in δR (the third term of equation (3)), with a term involving the adjoint flux Ψ^+ and (known) data permutations $\delta\alpha$. Doing so, the last term of δR of equation (3) can be rewritten as:

$$\delta R = \int_V \int_0^{t_f} [\Psi^+(\mathbf{r},t)]^T [L'_\alpha(\alpha^0;\delta\alpha)][\Psi(\mathbf{r},t)] d\mathbf{r}dt + \hat{\mathbf{P}} \quad (12)$$

The operator L' contains the perturbations $\delta\lambda_k, \delta\beta_k$ and $\delta\chi_{d,k}$ as they occur in the RHS of equations (8) and (9). The adjoint solution is found using the adjoint operator L^+, and the bilinear concommittant $\hat{\mathbf{P}}$ contains boundary terms associated with the adjoint operator(s) of L^+. Expression (12) contains only (known) data perturbations $\delta\alpha$, and can be easily solved once the adjoint solutions $\phi^+(\mathbf{r},t)$ and $C^+(\mathbf{r},t)$ have been determined.

2 Adjoint equations and the form of $\hat{\mathbf{P}}$

The adjoint solution $\Psi(\mathbf{r},t)$ obeys the operator that is adjoint to the LHS of (8) and (9) (ϕ^{g+}, C_k^+ are used to eliminate $\delta\phi^g, \delta C_k$ appearing in (8) and (9)). The adjoint equations thus become:

$$\frac{-1}{v^g}\frac{\partial \phi^{g+}}{\partial t} - \nabla \cdot D^g \nabla \phi^{g+} + \Sigma_t^g \phi^{g+} - \sum_{g'=1}^{G} \Sigma_s^{g \to g'} \phi^{g'+} - \ldots$$
$$\ldots - \nu^g \Sigma_f^g \sum_{g'=1}^{G} \chi_p^{g'} (1-\beta) \phi^{g'+} - \nu \Sigma_f^g \sum_{k=1}^{K} \beta_k C_k^+ = Q_\phi^+ \quad (13)$$

$$\frac{-\partial C_k^+}{\partial t} - \sum_{g=1}^{G} \chi_{d,k}^g \lambda_k \phi^{g+} + \lambda_k C_k^+ = Q_C^+ \quad (14)$$

We now turn our attention to the adjoint source Q^+ and the necessary boundary conditions. Since the adjoint equations are 'looking back' in time ($-\partial/\partial t$), the 'initial' conditions are set at the end of the calculation interval as 'final time conditions'. The spatial boundary conditions for the adjoint diffusion equation are the same as for the forward equation Ott and Neuhold [1985].

For the first implementation, a uniform, homogeneous reactor geometry was assumed. The power at some final time t_f is required. For the homogeneous reactor, the fission cross section is a constant and we can write for R:

$$R = E_{\text{rel}} \Sigma_f \int_V \int_0^{t_f} \phi(\mathbf{r}, t) \delta(t - t_f) dt d\mathbf{r} \quad (15)$$

From this equation it is seen that, without loss of generality, we can define R as $\iint \phi(\mathbf{r}, t)\delta(t - t_f)dtd\mathbf{r}$ for the homogeneous reactor, and equation (3) reduces to

$$\delta R = \int_V \int_0^{t_f} \delta\phi(\mathbf{r}, t) \delta(t - t_f) dt d\mathbf{r} \quad (16)$$

To determine the adjoint source Q^+, δR of equation (16) has to be written as a scalar product involving $\delta\phi$. Upon inspection, equation (16) is already in the form of a scalar product, and the adjoint source Q^+ is readily found to be:

$$\begin{aligned} Q_\phi^+ &= \delta(t - t_f) \\ Q_C^+ &= 0 \end{aligned} \quad (17)$$

For the adjoint of the $\partial/\partial t$-operator:

$$\int_0^{t_f} g^T(\mathbf{r}, t) D \frac{\partial f(\mathbf{r}, t)}{\partial t} dt = [g^T(\mathbf{r}, t) D f(\mathbf{r}, t)]_0^{t_f} - \int_0^{t_f} f^T(\mathbf{r}, t) D \frac{\partial g(\mathbf{r}, t)}{\partial t} dt \quad (18)$$

with D a diagonal matrix. From this equation, the adjoint of $\partial/\partial t$ is found as $-\partial/\partial t$, and the first term on the RHS of (18) is $\hat{\mathbf{P}}$, a term arising from taking the adjoint. From equation (18) we choose $\phi^{g+}(\mathbf{r}, t_f) = C_k^+(\mathbf{r}, t_f) = 0$, so that $\hat{\mathbf{P}}$ only contains terms at $t = 0$. In the ASAP, $g(t) = \Psi^+(t)$ and $f(t) = \delta\Psi(t)$. Now that we have chosen the final time condition $\Psi^+(t_f) = 0$, we can infer from equation (18) the form of $\hat{\mathbf{P}}$:

$$\hat{\mathbf{P}} = \int_V [\Psi^+(\mathbf{r}, 0)]^T [D][\delta\Psi(\mathbf{r}, 0)] d\mathbf{r} \tag{19}$$

where $\delta\Psi$ contains the $\delta\phi^g$- and δC_k-terms as they appear in equations (10) and (11). Note that the spatial part of equation (4) is formally self-adjoint and thus does not yield a contribution to $\hat{\mathbf{P}}$.

Now the adjoint source is known: $Q_\phi^+ = \delta(t - t_f), Q_C^+ = 0$. The final time conditions for the adjoint equations are $\phi^{g+}(\mathbf{r}, t_f) = C_k^+(\mathbf{r}, t_f) = 0$. The Dirac-delta in Q^+ can also be written as an equivalent final time condition. To do so, consider that the following system has to be solved:

$$-D\frac{\partial}{\partial t}\Psi^+(\mathbf{r}, t) = L^+\Psi^+(\mathbf{r}, t) + \delta(t - t_f) \tag{20}$$

with D the diagonal matrix containing $1/v^i$ for the neutron groups and 1 for the precursors. Using a Laplace transform, it is seen that the Dirac delta can be rewritten as a final condition Ψ_f^+ if $\Psi_f^{i+} = 1/D(i, i)$. With these equations, the adjoint system is fully defined and can be solved. Thus the Adjoint Sensitivity Analysis Procedure can be summarized as follows:

- Define the reference forward response R, and determine which parameters are to be perturbed.
- Define the forward operator L which yields the solution ϕ^0 appearing in R.
- To obtain the adjoint solution ϕ^+, determine the adjoint operator L^+. To solve for ϕ^+, set $Q^+ = \nabla_\phi R$.
- Determine the operator $L'(\alpha^0; \delta\alpha)$, i.e. the operator containing the data perturbations.
- Calculate the scalar products and $\hat{\mathbf{P}}$ appearing in equation (12), and δR is known.

3 Calculations without spatial dependence

To gain experience with the ASAP and gain insight into the structure of the equations, an infinite homogeneous reactor was simulated using the numerical software Scilab (INRIA ENPC [2006]). For the infinite medium calculation, there is no spatial dependence for the diffusion equation, and the problem can be directly integrated using the ODE-functions of Scilab. The reactor under consideration is GFR-600, a 600 MWth Gas Cooled Fast Reactor currently researched within the European Sixth Framework Program GCFR-STREP. GFR-600 is a helium-cooled reactor, with a matrix fuel containing 70% UPuC and 30% SiC in plate form. Cladding and structural materials are SiC.

Cell-mixed cross-sections were prepared for a representative GFR-600 fuel mixture using the CSAS-sequence of SCALE 5 (ORNL [2005]). The original 172 group data are condensed to an 8-group fast reactor

Table I. Values of λ_k and β_k for infinite homogeneous medium calculations.

Prec. gr.	1	2	3	4	5	6
λ_k	1.29e-02	3.11e-02	1.34e-01	3.31e-01	1.26e+00	3.21e+00
β_k	1.173e-04	7.119e-04	6.825e-04	1.228e-03	3.501e-04	1.370e-04

Table II. The delayed neutron spectrum, χ_d, for infinite homogeneous medium calculations.

Neut. gr.	1	2	3	4
χ_d	1.780e-02	3.217e-01	3.454e-01	2.404e-01
	5	6	7	8
χ_d	4.178e-02	2.822e-02	4.163e-03	4.682e-04

structure as given in Waltar and Reynolds [1981]. The fissile enrichment was set to give a k_{eff} slightly higher than 1.0. The delayed neutron parameters are obtained from the VAREX program (Kloosterman and Kuijper [2000]). A Scilab-script was prepared to obtain the reference solution $\Psi^0(t)$, the adjoint solution $\Psi^+(t)$, and to also perform a perturbed calculation giving $\Psi(t)$. Tables I and II list the values of λ_k, β_k and χ_d used in the calculations.

At first, note that a change of response δR due to initial conditions without any data perturbations can only arise from the $\hat{\mathbf{P}}$-term (19). This property can be used to check whether the adjoint $\Psi^+(t)$ is correctly solved (no data perturbations are involved, hence δR due to initial conditions is exact). It was found that $\Psi(t)$ and $\Psi^+(t)$ can be solved with quite coarse time sampling without loss of accuracy. However, if those solutions are used to calculate δR due to data perturbations, the results are inaccurate. This is due to the coarse 'sampling' of $\Psi(t)$ and $\Psi^+(t)$, in which much 'detail' is lost by the large time steps. For example, the forward solution will show a prompt jump at the onset of the transient, leading to the requirement of fine time sampling for $t = 0$. For the adjoint solutions, a similar behaviour exists for both the neutrons fluxes and precursor concentrations at t_f, requiring a very fine time sampling near the final time t_f.

Calculations were performed for a very slow transient ($\rho = 0.02\$$) over a period of 100 s. $\Psi(t)$ and $\Psi^+(t)$ were calculated on separate time-grids, with a logarithmic stepping and very small steps for the crucial parts of the transients near $t = 0$ and $t = t_f$. The solutions are subsequently re-gridded to a common time grid to calculate the scalar products (equation (12)). An example of $\phi^{i+}(t)$ and $C_k^+(t)$ are given in figures 1 and 2. Note the shape of $C_k^+(t)$. For the slowest delay group ($\lambda = 0.0129$ s^{-1}) the adjoint is steadily decreasing, while the fastest delay group ($\lambda = 3.21$ s^{-1}) is more or less constant but increases towards the end of the transient. This can be interpreted as follows: the adjoint $C_k^+(t)$ is a measure of the contribution of one precursor to the final neutron population. If a slowly decaying precursor is added to the reactor, it will 'not have time' to decay and the resulting neutron will not contribute to R. For a quickly decaying precursor, its contribution will only be important towards the end of the interval. For very long times before the end of the interval, all adjoint precursor concentrations are equal, as each precursor adds one neutron to the population. In a (slightly) supercritical reactor the added neutron will multiply, hence the adjoint precursor concentrations are slightly higher at the beginning of the interval if $\rho > 0$. For $\rho < 0$ the opposite is true, as illustrated in figure 3.

In tables III and IV sensitivity profiles are given for all delayed neutron parameters in $\%\delta R$ / $\%\delta\alpha$ for this transient. This table also lists the result of a direct, perturbed calculation. It is seen from the table, that the

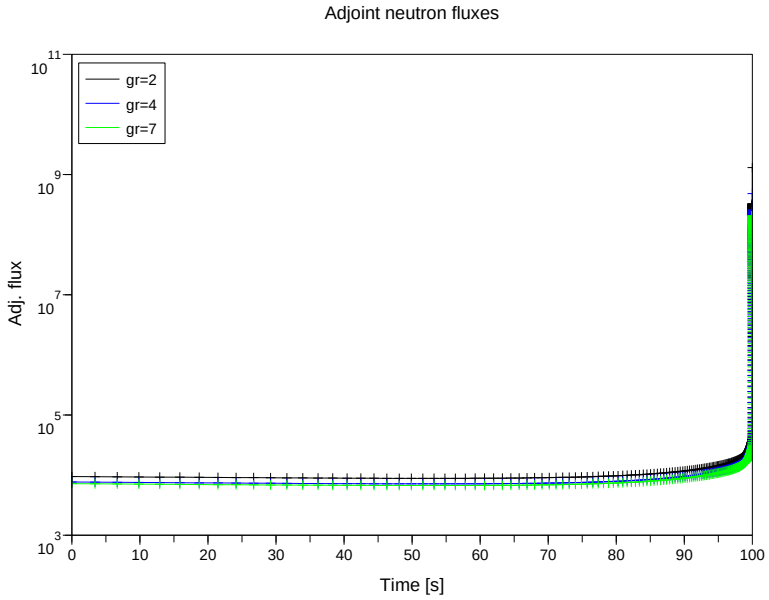

Figure 1. Adjoint neutron fluxes for a transient with $\rho > 0$. Note the logarithmic y-axis. Due to the rapid increase at the end of the time window, a proper time sampling is crucial.

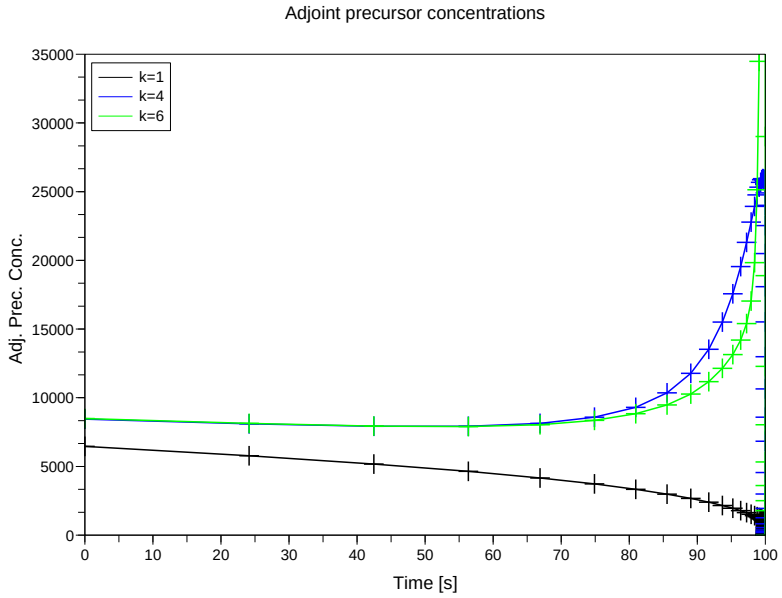

Figure 2. Adjoint precursor concentrations for a transient with $\rho > 0$. Like in figure 1, proper time sampling is crucial at the end of the time interval.

ASAP performs quite well, except when δR is small. Note that the largest sensitivities are for $\chi_{d,2}$, λ_2 and β_4. The sensitivity to λ_2 is somewhat surprising for a positive transient. This will be discussed later.

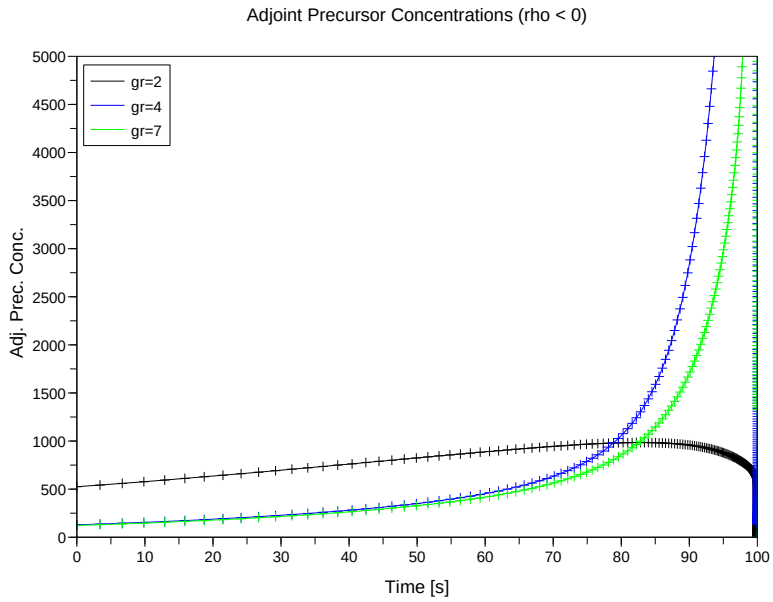

Figure 3. Adjoint precursor concentrations for a transient with $\rho < 0$. Adding extra precursors at the beginning of the interval only increases the response R slightly, because the neutrons produced by the precursors will not all contribute to R.

By the nature of our calculations, the data sensitivities depend on the type of transient under consideration. Therefore, the ASAP was employed to analyse a set of transients with different reactivities. For instance, it may be a assumed a-priori that a decreasing transient is most sensitive in the long run to λ_1, the slowest decaying precursor group. In tables V, VI and VII the sensitivities are given for 6 transients, three transients with increasingly positive reactivity, and 3 transients with increasingly negative reactivity. As a measure of how rapidly the neutron flux increases or decreases the ratio $R_p = \sum_{g=1}^{G} \phi^g(t_f) / \sum_{g=1}^{G} \phi^g(0)$ is used.

Interpreting the results in tables V, VI and VII it is seen that for increasingly positive reactivities all sensitivities increase, and that the relative sensitivities tend to increase for the precursor groups with short time scales (groups 1 and 2). This is to be expected, because the more one approaches the margin of prompt criticality, the larger the effect of small changes of β_k, λ_k. The effects of variations of the delayed spectrum are less dependent on reactivity, as expected, because this term merely distributes neutrons over energy groups,

Table III. Sensitivity of a slow transient to delayed neutron parameters. ASAP = Adjoint Sensitivity Analysis Procedure, FSAP = Forward Sensitivity Analysis Procedure, i.e. a direct calculation with perturbed data. All numbers given as %/%. The ASAP gives adequate results for this transient.

Prec. gr.	1	2	3	4	5	6
S_{λ_k} ASAP	1.861e-02	1.160e-01	4.280e-02	3.415e-02	2.835e-03	4.969e-04
S_{λ_k} FSAP	1.846e-02	1.151e-01	4.198e-02	3.299e-02	2.562e-03	3.966e-04
S_{β_k} ASAP	-1.577e-01	-8.516e-01	-7.050e-01	-1.221e-00	-3.410e-01	-1.327e-01
S_{β_k} FSAP	-1.570e-01	-8.406e-01	-6.992e-01	-1.208e-00	-3.395e-01	-1.324e-01

Table IV. Sensitivity of a slow transient to the delayed neutron spectrum, χ_d. ASAP = Adjoint Sensitivity Analysis Procedure, FSAP = Forward Sensitivity Analysis Procedure, i.e. a direct calculation with perturbed data. All numbers given as %/%. The ASAP gives adequate results for this transient.

Neut. gr.	1	2	3	4
S_{χ_d} ASAP	9.283e-02	4.326e-01	-1.196e-01	-2.553e-01
S_{χ_d} FSAP	9.277e-02	4.331e-01	-1.194e-01	-2.545e-01
	5	6	7	8
S_{χ_d} ASAP	-8.315e-02	-6.103e-02	-7.148e-03	4.421e-04
S_{χ_d} FSAP	-8.302e-02	-6.093e-02	-7.136e-03	4.433e-04

Table V. Sensitivities for λ_k and β_k for three transients with increasingly positive reactivity.

	R_p = 1.32e+00		R_p = 2.99e+00		R_p = 8.68e+00	
k	S_{λ_k}	S_{β_k}	S_{λ_k}	S_{β_k}	S_{λ_k}	S_{β_k}
1	1.861e-04	-1.577e-03	6.350e-04	-3.262e-03	1.044e-03	-5.538e-03
2	1.160e-03	-8.516e-03	4.369e-03	-1.604e-02	7.985e-03	-2.711e-02
3	4.280e-04	-7.050e-03	1.975e-03	-1.073e-02	4.511e-03	-1.655e-02
4	3.415e-04	-1.221e-02	1.652e-03	-1.705e-02	4.047e-03	-2.442e-02
5	2.835e-05	-3.410e-03	1.343e-04	-4.503e-03	3.401e-04	-6.064e-03
6	4.969e-06	-1.327e-03	2.152e-05	-1.729e-03	5.407e-05	-2.290e-03

Table VI. Sensitivities for λ_k and β_k for three transients with increasingly negative reactivity.

	R_p = 6.95e-01		R_p = 5.76e-02		R_p = 3.49e-03	
k	S_{λ_k}	S_{β_k}	S_{λ_k}	S_{β_k}	S_{λ_k}	S_{β_k}
1	-2.724e-04	-3.279e-04	-3.118e-03	3.426e-03	-5.912e-03	4.875e-03
2	-1.553e-03	-3.479e-03	-1.151e-02	6.503e-03	-1.509e-02	5.488e-03
3	-4.673e-04	-4.716e-03	-1.154e-03	-2.565e-04	-1.678e-04	2.695e-05
4	-3.454e-04	-8.999e-03	-7.134e-04	-1.609e-03	-8.649e-05	-1.125e-04
5	-2.440e-05	-2.640e-03	-4.785e-05	-6.051e-04	-3.859e-06	-5.107e-05
6	-3.171e-06	-1.039e-03	-6.644e-06	-2.485e-04	-1.047e-06	-2.147e-05

Table VII. Sensitivities for χ_d, for all transients. Left: increasingly positive reactivity, right: increasingly negative reactivity.

	R_p = 1.32	R_p = 2.99	R_p = 8.68	R_p =0.695	R_p =0.0576	R_p = 0.00349
k	S_{χ_d}	S_{χ_d}	S_{χ_d}	S_{χ_d}	S_{χ_d}	S_{χ_d}
1	9.283e-04	1.123e-03	1.371e-03	7.777e-04	2.922e-04	1.103e-04
2	4.326e-03	5.234e-03	6.391e-03	3.624e-03	1.362e-03	5.162e-04
3	-1.196e-03	-1.446e-03	-1.765e-03	-1.002e-03	-3.759e-04	-1.376e-04
4	-2.553e-03	-3.089e-03	-3.771e-03	-2.139e-03	-8.048e-04	-3.118e-04
5	-8.315e-04	-1.006e-03	-1.229e-03	-6.964e-04	-2.612e-04	-9.749e-05
6	-6.103e-04	-7.385e-04	-9.019e-04	-5.111e-04	-1.917e-04	-7.177e-05
7	-7.148e-05	-8.650e-05	-1.057e-04	-5.986e-05	-2.247e-05	-8.608e-06
8	4.421e-06	5.348e-06	6.526e-06	3.703e-06	1.376e-06	3.948e-07

but does not control the production rate of delayed neutrons, as the other parameters do.

For the negative transients, the general trend for the sensitivities is less clearly defined. For rapidly decreasing transients, the sensitivities tend to increase for the slowly decaying groups (λ_1 and λ_2) and decrease for the other groups. Notice that some sensitivities for β_k change sign for decreasing transients. A full explanation for this effect is under investigation. It may be surprising that even for negative reactivities the largest sensitivity does not occur for λ_1. This can be justified by the value of the asymptotic reactor period as derived from the inhour-equations. In Ott and Neuhold [1985] the following value is given:

$$\lambda_{as} = \frac{\beta}{\sum_{k=1}^{K} \frac{\beta_k}{\alpha' + \lambda_k}} - \alpha' \tag{21}$$

with α' a constant dependent on the reactivity of the reactor. Thus λ_{as} depends on all delay groups, not just on the slowest (or the fastest) decaying group. Thus for both positive and negative reactivities, the largest sensitivities may not occur for the fastest and slowest decay groups, as may be a priori expected. The sensitivity for the delayed neutron spectrum varies slower than the sensitivity for λ_k and β_k for the 6 transients.

4 Implementation in the code DALTON

The Adjoint Sensitivity Analysis Procedure requires solution of the 'reference' forward flux ϕ_0, and determination of the 'reference' response R_0, as well as determination of the adjoint solution ϕ_0^+. This is done using the special purpose code DALTON. DALTON solves the multigroup diffusion equations on a structured grid (xyz or $rz\theta$ coordinates). A finite volume technique is used for discretizing the equations in space and an Euler implicit technique is applied for time-discretization. The code can handle both the fundamental and higher lambda and time-eigenvalues as well as time-stepping in forward and adjoint mode. The higher eigenmodes are obtained by the use of the ARPACK package. Linear systems arising from discretization are solved using preconditioned CG. In the multigroup case, acceleration of the Gauss-Seidel group by group solution procedure is obtained by the techniques introduced by Adams and Morel [1993] and Morel and McGhee [1994]. Another option available is to use a multi-group Krylov technique where the preconditioner consists of the accelerated Gauss-Seidel procedure.

In the implicit Euler scheme the time-dependent diffusion or transport equation is rewritten as a fixed source calculation. In table VIII the sets of equations for the forward and adjoint problem are given. It is seen that in order to calculate the adjoint fluxes, apart from trivial changes of the scatter and fission operators, only the (time-dependent) source $q'^{i+}_{[n]}$ and the equation for the adjoint precursor concentrations $C^+_{k,[n+1]}$ are different from the forward case. Because the adjoint is defined by $-\partial/\partial t$ (equations (13) and (14)), the result from DALTON needs to be reversed in time for the subsequent analysis.

For this research the adjoint time stepping option was built into DALTON. DALTON saves all fluxes to files, which are read by a separately written post-processing program. Since the adjoint is solved 'backward' in time, it is unfortunately not possible to calculate $\Psi(t)$ and $\Psi^+(t)$ and calculate the scalar products in one DALTON run. For DALTON, a cylindrical reactor with $H = D = 2$ m is assumed, with vacuum boundary conditions on all surfaces. The reactor is assumed to be homogeneous. Again, cross sections were prepared in 8 groups with CSAS to give a k_{eff} slightly larger than 1.0. The current version of DALTON allows time

Table VIII. Forward and Adjoint equation sets for the Implicit Euler discretized calculations

Implicit Euler for $\Psi(t)$	Implicit Euler for $\Psi(t)^+$
$(-\nabla \cdot D(\mathbf{r})\nabla + \Sigma_t^{'g}(\mathbf{r}))\phi^g_{[n+1]}(\mathbf{r}) = \ldots + \sum_{g'=1}^{G} \Sigma_s^{g'\rightarrow g}(\mathbf{r})\phi^{g'}_{[n+1]}(\mathbf{r}) + \ldots + \chi^{'g}\sum_{g'=1}^{G}\nu\Sigma_f^{g'}(\mathbf{r})\phi^{g'}_{[n+1]}(\mathbf{r}) + \ldots + q^{'g}_{[n]}(\mathbf{r})$ (22)	$(-\nabla \cdot D(\mathbf{r})\nabla + \Sigma_t^{'g}(\mathbf{r}))\phi^{g+}_{[n+1]}(\mathbf{r}) = \ldots + \sum_{g'=1}^{G} \Sigma_s^{g\rightarrow g'}(\mathbf{r})\phi^{g'+}_{[n+1]}(\mathbf{r}) + \ldots + \nu\Sigma_f^{g}(\mathbf{r})\sum_{g'=1}^{G}\chi^{'g'}\phi^{g'+}_{[n+1]}(\mathbf{r}) + \ldots + q^{'g+}_{[n]}(\mathbf{r})$ (23)
$\Sigma^{'g}_{t,[n]} = \Sigma^g_t + \frac{1}{v^g \Delta t_{[n]}}$ (24)	$\Sigma^{'g}_{t,[n]} = \Sigma^g_t + \frac{1}{v^g \Delta t_{[n]}}$ (25)
$\chi^{'g} = \chi^g_p(1-\beta) + \sum_{k=1}^{K}\chi^g_{d,k}\lambda_k\gamma_k\beta_k$ (26)	$\chi^{'g} = \chi^g_p(1-\beta) + \sum_{k=1}^{K}\chi^g_{d,k}\lambda_k\gamma_k\beta_k$ (27)
$q^{'g}_{[n]}(\mathbf{r}) = \sum_{k=1}^{K}\chi^g_{d,k}\lambda_k\gamma_k\frac{C_{k,[n]}(\mathbf{r})}{\Delta t} + \frac{\phi^g_{[n]}(\mathbf{r})}{v^g\Delta t_{[n]}} + q^g_{\text{ext}}[n]$ (28)	$q^{'g+}_{[n]}(\mathbf{r}) = \nu\Sigma^g_f(\mathbf{r})\sum_{k=1}^{K}\beta_k\gamma_k\frac{C^+_{k,[n]}(\mathbf{r})}{\Delta t} + \frac{\phi^{g+}_{[n]}(\mathbf{r})}{v^g\Delta t_{[n]}} + q^{g+}_{\text{ext}}[n]$ (29)
$C_{k,[n+1]}(\mathbf{r}) = \gamma_k\beta_k\sum_{g'=1}^{G}\nu\Sigma_f^{g'}(\mathbf{r})\phi^{g'}(\mathbf{r}) + \gamma_k\frac{C_{k,[n]}(\mathbf{r})}{\Delta t_{[n]}}$ (30)	$C^+_{k,[n+1]}(\mathbf{r}) = \gamma_k\sum_{g'=1}^{G}\chi^{g'}_{d,k}\lambda_k\phi^{g'+}(\mathbf{r}) + \gamma_k\frac{C^+_{k,[n]}(\mathbf{r})}{\Delta t_{[n]}}$ (31)
$\gamma_k = [\frac{1}{\Delta t_{[n]}} + \lambda_k]^{-1}$ (32)	$\gamma_k = [\frac{1}{\Delta t_{[n]}} + \lambda_k]^{-1}$ (33)

Table IX. Values of λ_k and β_k for the GFR-600 calculations with DALTON. Differences between β_k values reported here and in table I are due to the difference of spectrum between the finite and infinite homogeneous medium calculations.

Prec. gr.	1	2	3	4	5	6
λ_k	1.29e-02	3.11e-02	1.34e-01	3.31e-01	1.26e+00	3.21e+00
β_k	1.145e-04	6.947e-04	6.661e-04	1.199e-03	3.416e-04	1.336e-04

Table X. The delayed neutron spectrum, χ_d, for finite homogeneous medium calculations. Difference between these data and those presented in table II are due to spectral differences between the finite and infinite medium calculations.

Neut. gr.	1	2	3	4
χ_d	1.781e-02	3.217e-01	3.454e-01	2.404e-01
	5	6	7	8
χ_d	4.178e-02	2.822e-02	4.163e-03	4.635e-04

stepping with a fixed Δt only. To assure a fine enough time-stepping, 1000 steps were taken with Δt = 5.0e-6 s (it is possible to take more steps, but since all fluxes are to be saved for both the forward and the adjoint fluxes at each time step, the amount of data to be post-processed increases rapidly beyond manageable amounts). The spatial meshing is 21 nodes in both r-direction and z-direction, thus giving 21 x 21 nodes, with 14 fluxes (8 neutron groups and 6 precursor groups) to be calculated in each node at each time step. The values of β_k, λ_k and the delayed neutron spectrum χ_d are given in tables IX and X for reference.

Since the code is still under development, an option to do a direct calculation with perturbed data has also been implemented. In table XI an example of a DALTON + post-processor run is given for some arbitrary data perturbations. Again, the ASAP performs remarkably well if the time stepping is fine enough and the data perturbations are small.

An option to calculate the sensitivity profile for the delayed neutron parameters was also implemented into the post-processor. The result for the transient described earlier is given in table XII. It should be noted, however, that the sensitivities are probably not very accurate because the transient is very short. Infinite medium calculations with Scilab have confirmed that especially the sensitivity to λ_k is not accurate if the transient is short compared to the values of λ_k.

5 Conclusions and future work

In this paper a theoreticalal framework based on the Adjoint Sensitivity Analysis Procedure (ASAP) has been derived to calculate the sensitivities of a transient in a nuclear reactor to delayed neutron parameters. The current approach does not include feedback effects. The theoretic framework has been applied to a 600 MWth Generation IV Gas Cooled Fast Reactor. Concluding:

- The time sampling is crucial, especially at the boundaries of the time interval. The adjoint solution is especially sensitive to the time sampling.

Table XI. . Result of Adjoint Sensitivity Analysis Procedure and Forward Sensitivity Analysis Procedure for a 3-D cylindrical reactor geometry using the DALTON code and post-processor. Some arbitrary data perturbations are input. The ASAP and FSAP results are in good agreement, so it is concluded that time-stepping etc. is fine enough with the applied settings.

k	$\delta\lambda_k$	$\delta\beta_k$	g	$\delta\chi_d$
1	-2%	-3%	1	0
2	-1%	-2%	2	0
3	-4%	-3%	3	5%
4	2%	1%	4	0
5	-4%	-3%	5	0
6	-2%	-3%	6	0
			7	0
			8	0
$\delta\phi(\mathbf{r},0)$				2%
δR ASAP	0.022714			
δR FSAP	0.022757			

Table XII. Sensitivity profile for λ_k and β_k calculated with DALTON and post-processor for a bare cylindrical reactor. The accuracy of the sensitivities for λ_k is probably not very good because the transient is very short.

Prec. gr.	1	2	3	4	5	6
S_{β_k}	-1.076e-04	-6.526e-04	-6.257e-04	-1.126e-03	-3.209e-04	-1.254e-04
S_{λ_k}	1.032e-05	6.261e-05	6.004e-05	1.081e-04	3.089e-05	1.214e-05

Table XIII. Sensitivity profile for χ_d for a bare, cylindrical reactor using DALTON and post-processor.

Neut. gr.	1	2	3	4
S_{χ_d}	3.790e-04	1.703e-03	-4.544e-04	-1.015e-03
	5	6	7	8
S_{χ_d}	-3.436e-04	-2.492e-04	-2.899e-05	2.231e-06

- For problems without spatial dependence, the ASAP has been shown to give accurate results for all perturbations of λ_k, β_k and χ_d.
- For slow positive transients in the reactor under consideration, the largest sensitivies occur for λ_2, β_4 and $\chi_{d,2}$.
- For rapid positive transients, the largest sensitivies occur for λ_2, β_2 and $\chi_{d,2}$.
- For negative transients, the largest sensitivies occur for λ_2, β_2 and $\chi_{d,2}$.
- For calculations with spatial dependence, the ASAP also gives accurate results, if the spatial and time meshing are fine enough.

The Scilab calculations have shown that both forward and adjoint solution can be obtained with good enough accuracy with quite coarse time sampling. However, to be able to accurately the scalar products, the time-sampling near the boundaries of the interval needs to be fine enough. To make DALTON capable of treating realistic transients in 3-D, it is necessary to introduce a variable time step Δt. In this way, the amount of data to be post-processed remains manageable.

The big advantage of the ASAP for delayed neutron parameters is that it can be implemented as a post-processor to any general code capable of calculating time dependent forward and adjoint fluxes, provided that the time stepping is accurate enough.

ACKNOWLEDGEMENTS

The authors acknowledge the support of the European Commission. The GCFR STREP is carried out under Contract Number 012773 (FI6O) within the EURATOM 6th Framework Programme, effective from March 1st 2005 to February 28th 2009 (http://www.cordis.lu/fp6/). Please visit our website at htpp://www.gcfr.org.

REFERENCES

E. Kiefhaber. Influence of delayed neutron spectra on fast reactor criticality. *Nuclear Science and Engineering*, 111:197–204, 1992.

R.J. Onega and R.J. Florian. The implication of sensitivity analysis on the safety and delayed neutron parameters for fast breeder reactors. *Annals of Nuclear Energy*, 10:477–490, 1983.

C. de Oliveira and A. Goddard. EVENT - A multidimensional finite element-spherical harmonics radiation transport code. In *Proc. Int. Seminar 3-D Deterministic Radiation Transport Codes*, Paris, France, 1996. OECD.

A. Pautz and A. Birkhofer. DORT-TD: A transient neutron transport code with fully implicit time integration. *Nuclear Science and Engineering*, 145:299–319, 2003.

D.G. Cacuci. *Sensitivity and uncertainty analysis*, volume I, Theory. CRC Press, 2003.

W.F.G. van Rooijen. *Improving fuel cycle design and safety characteristics of a Gas Cooled Fast Reactor*. PhD thesis, Delft University of Technology, The Netherlands, 2006. IOS Press Amsterdam for Delft University Press, available online through http://repository.tudelft.nl/.

W.F.G. van Rooijen, J.L. Kloosterman, T.H.J.J. van der Hagen, and H. van Dam. Definition of breeding gain for the closed fuel cycle and application to a gas cooled fast reactor. *Nuclear Science and Engineering*, 2007. Accepted for publication.

K.O. Ott and R.J. Neuhold. *Introductory Nuclear Reactor Dynamics*. ANS, 1985.

INRIA ENPC. *Scilab, the open source platform for numerical computation*. Copyright © 1989-2005., 2006.

ORNL. *SCALE: A modular code system for performing standardized computer analyses for licensing evaluations, ORNL/TM-2005/39, version 5, Vols I-III*. Oak Ridge National Laboratory, April 2005. Available from Radiation Safety Information Computational Center at Oak Ridge National Laboratory as CCC-725.

A.E. Waltar and A.B. Reynolds. *Fast Breeder Reactors*. Pergamon Press, 1981.

J.L. Kloosterman and J.C. Kuijper. VAREX, a code for variational analysis of reactivity effects: description and examples. In *PHYSOR 2000*, Seoul, South Korea, October 7-10 2000. ANS.

B.T. Adams and J.E. Morel. 'a two-grid acceleration scheme for the multigroup S_n equations with neutron upscattering. *Nuclear Science and Engineering*, 115:253–264, 1993.

J.E. Morel and J.M. McGhee. A fission-source acceleration technique for time-dependent even-parity S_n calculations. *Nuclear Science and Engineering*, 116:73–85, 1994.